Biomaterials Science

ROYAL SOCIETY OF CHEMISTRY

PAPER

View Article Online
View Journal | View Issue

Cite this: *Biomater. Sci.*, 2026, **14**, 2125

Ciprofloxacin–polymer conjugates targeted with iron(III) for effective treatment of intracellular bacterial infections

Anna Stehlíková, Lenka Kotrchová, Michal Pechar, Kristýna Gunár, Eliška Rydvalová, Martin Studenovský and Tomáš Etrych *

The increasing prevalence of multidrug-resistant bacteria necessitates innovative antibiotic strategies beyond the discovery of new active compounds. Here, we report *N*-(2-hydroxypropyl)methacrylamide (HPMA)-based polymer–ciprofloxacin conjugates combining controlled drug release with siderophore-mediated targeting *via* a deferoxamine–Fe^{3+} (DFX–Fe) complex. The conjugates differed in linker type (non-cleavable amide *vs.* reductively cleavable disulfide) and in the presence of the DFX–Fe targeting unit. Non-cleavable conjugates showed strongly reduced antibacterial activity, whereas disulfide-linked systems enabled the release of chemically intact and biologically active ciprofloxacin under reducing conditions. DFX–Fe targeting significantly enhanced the efficacy of non-cleavable conjugates, while modulating drug release kinetics in cleavable systems due to the redox activity of Fe^{3+}. Antibacterial activity against *Escherichia coli* and *Staphylococcus aureus* strongly depended on the conjugate structure and bacterial species. Importantly, in a macrophage intracellular infection model, stimuli-responsive conjugates exhibited high bactericidal activity, reducing intracellular bacteria to below 1% at a 2× MIC concentration. This observation indicates the great potential of these nanotherapeutics in the treatment of challenging bacterial infections. All systems showed good biocompatibility toward human fibroblasts. Overall, this study highlights the critical roles of linker cleavability and siderophore-mediated targeting in the design of polymeric antibiotics for intracellular bacterial infections.

Received 30th January 2026,
Accepted 4th March 2026

DOI: 10.1039/d6bm00145a

rsc.li/biomaterials-science

1. Introduction

The increasing prevalence of multidrug-resistant bacterial strains represents one of the greatest challenges for modern medicine.[1,2] Traditional strategies based on the discovery of new antibiotics face limitations in the rate of innovation and high development costs, while multidrug resistance (MDR) often emerges shortly after the introduction of a new agent into clinical practice.[3] As a result, growing attention has been directed toward alternative approaches that do not rely on entirely new molecules but instead on innovative delivery systems for existing antibiotics, with the goal of enhancing their efficacy and prolonging their clinical lifetime.[4,5]

One such approach is the conjugation of antibiotics with water-soluble polymers.[6,7] Polymer–drug conjugates offer several advantages, including improved solubility and stability of the active compound, a prolonged circulation half-life, the ability to accumulate at the site of infection, and, importantly, the possibility of controlled drug release.[8] A key parameter is the nature of the linkage between the antibiotic and the polymer carrier. While non-cleavable linkages typically result in permanent inactivation of the drug, the introduction of cleavable linkers, particularly disulfide bonds, enables selective release of the active molecule within the reducing environment of the bacterial cytoplasm.[9]

Ciprofloxacin (Cip) is a fluoroquinolone antibiotic with broad-spectrum activity against both Gram-positive and Gram-negative bacteria.[10,11] Although ciprofloxacin remains a cornerstone of clinical practice, the increasing prevalence of MDR and its limited intracellular penetration in certain pathogens restrict its therapeutic effectiveness.[12,13] Conjugation of ciprofloxacin to a polymer carrier through an appropriately designed linker therefore provides a promising strategy to overcome these limitations while preserving biological activity.[14]

Another strategy to enhance antibiotic efficacy is siderophore-mediated transport.[15,16] Bacteria have evolved sophisticated mechanisms to acquire iron from their environment, producing siderophores—low-molecular-weight Fe^{3+} chelators—that are actively imported by specific membrane transporters.[17] This pathway offers a "Trojan horse" mechanism for tar-

Institute of Macromolecular Chemistry, Czech Academy of Sciences, Heyrovského nám. 2, Prague 6, Czech Republic. E-mail: etrych@imc.cas.cz; Tel: +420-296809231

geted antibiotic delivery.[18] However, most natural siderophores are species-specific, which limits their broader application. Deferoxamine (DFX), a clinically used iron chelator, is in contrast recognized as a xenosiderophore, internalized by transport systems of a wide range of bacterial species.[19] Owing to this universality, DFX–Fe is a suitable candidate for targeting polymer conjugates, enabling efficient intracellular uptake across diverse pathogens.

By combining ciprofloxacin and DFX–Fe in a polymer-based system (Fig. 1), a multifunctional therapeutic conjugate can be designed: the polymer carrier provides prolonged circulation and controlled release, while the targeting unit enhances intracellular uptake across a broad spectrum of bacteria.[19] Such systems hold potential clinical utility, for example, in the treatment and post-therapy of sepsis,[20] where sustained antibiotic exposure without frequent administration and minimized side effects are highly desirable.

The aim of this study was the design, synthesis, and comprehensive characterization of *N*-(2-hydroxypropyl)methacrylamide (HPMA)-based polymer–ciprofloxacin conjugates differing in the type of bond between the antibiotic and the polymer (cleavable *vs.* non-cleavable) and the presence of a DFX–Fe targeting unit. The study focuses on evaluating the impact of these parameters on drug release behavior, the antibacterial activity of the conjugates, and differences in efficacy against model representatives of Gram-positive *Staphylococcus aureus* (*S. aureus*) and Gram-negative *Escherichia coli* (*E. coli*) bacteria.

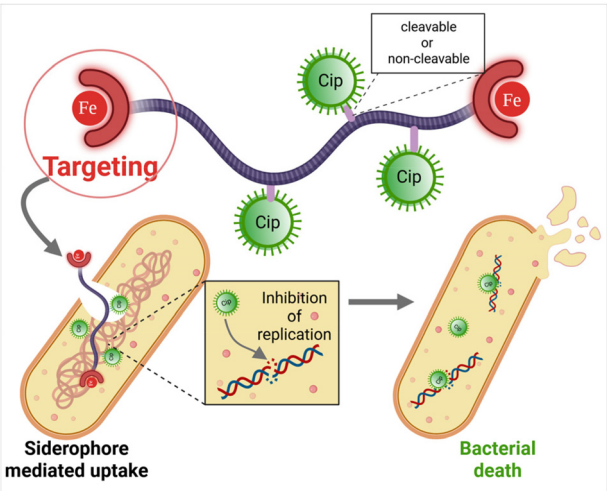

Fig. 1 Schematic illustration of the concept and the anticipated mode of action of the HPMA copolymer–ciprofloxacin conjugates bearing the DFX–Fe unit. Ciprofloxacin (Cip) is attached to the polymer backbone either through a reducible disulfide linker (cleavable conjugate) or *via* a stable non-cleavable linkage. The DFX–Fe moiety is designed to mimic bacterial siderophores and promote interaction of the conjugate with bacterial cells. After contact with the bacterial surface and/or in the surrounding reducing environment, ciprofloxacin may be released from the cleavable conjugate and inhibit bacterial DNA replication, leading to bacterial cell death.

2. Experimental section

2.1. Materials

tert-Butyl *N*-[2-(2-hydroxyethyldisulfanyl)ethyl]carbamate (Boc-NH-SS) and 2-(2-(9-9*H*-fluoren-9-ylmethyl *N*-[2-(2-hydroxyethyldisulfanyl)ethyl]carbamate)) (Fmoc-NH-SS) were purchased from Iris Biotech. *N*-(1,4,12,15,23,26,34-Heptaoxo-5,11,16,22,27,33-hexaaza-11,22,33-trihydroxypentatriacontane)-5-azadibenzocyclooctyne (DFX–DBCO) was purchased from Macrocyclics. Ciprofloxacin (Cip), iron(III) chloride hexahydrate ($FeCl_3 \cdot 6H_2O$), diisopropylethylamine (DIPEA), tetramethylurea (TMU), trifluoroacetic acid (TFA), dimethylformamide (DMF), dimethylacetamide (DMA), methanol (MeOH), dichloromethane (DCM), *tert*-butanol (*t*-BuOH), acetone, diethyl ether, tris(2-carboxyethyl)phosphine (TCEP), reduced glutathione (GSH), tris(hydroxymethyl)aminomethane hydrochloride (Tris-HCl), and all other reagents and solvents were purchased from Merck and used as received unless stated otherwise.

2.2. Synthesis of the disulfide ciprofloxacin derivative (SSCip)

The compound 7-[4-[2-(2-aminoethyldisulfanyl)ethoxycarbonyl]piperazin-1-yl]-1-cyclopropyl-6-fluoro-4-oxo-quinoline-3-carboxylic acid (**SSCip**) was synthesized *via* a three-step procedure without isolation of intermediates (Fig. 2). Only the final product **SSCip** was isolated and characterized.

SSCip derivatives were synthesized *via* two different approaches using either Fmoc or Boc protecting groups. The derivative obtained from Boc-NH-SS was synthesized according to the following procedure: Boc-NH-SS (99.2 mg, 3.9×10^{-4} mol) was reacted with phosgene in toluene (2 mL, 20% solution) at 25 °C for 10 h. After evaporation of the solvents and redissolution in DCM (3 mL), ciprofloxacin (129.1 mg, 3.9×10^{-4} mol) in TMU (3.5 mL) and DIPEA (81.9 μL, 4.7×10^{-4} mol) were added. The reaction was continued for 12 h at 25 °C. For removal of the Boc protecting group, TMU was evaporated and TFA (4 mL) was added. The mixture was purified by preparative HPLC to obtain **SSCip** as a TFA salt (140 mg, 70.3%). An alternative synthetic approach starting from Fmoc-NH-SS was also evaluated; however, it resulted in significantly lower yields and was therefore not pursued further. The structure and purity of **SSCip** were confirmed by ^{1}H NMR spectroscopy.

^{1}H NMR (400 MHz, *d*6-DMSO): δ = 1.18 (m, 2H, CH_2-cyclopropyl); 1.32 (m, 2H, CH_2-cyclopropyl); 2.93 (t, 2H, CH_2S); 3.03 (t, 2H, CH_2S); 3.11 (m, 2H, CH_2N-linker); 3.33 (m, 4H, CH_2N-piperazine); 3.62 (m, 4H, CH_2N-piperazine); 3.82 (septet, 1H, CH-cyclopropyl); 4.30 (t, 2H, CH_2O-linker); 7.58 (d, 1H, arom); 7.87 (br, 3H, NH_3^+); 7.94 (d, 1H, arom-CHCF); 8.68 (s, 1H, arom-CHN); 15.17 (br, 1H, COOH) ppm (Fig. S1)) The ^{13}C NMR spectrum and HRMS data of **SSCip** are provided in the SI (Fig. S2 and S3).

2.3. Synthesis of the monomers

HPMA and 3-(3-methacrylamido-propanoyl)thiazolidine-2-thione (Ma-β-Ala-TT) were synthesized according to previously reported procedures.[21]

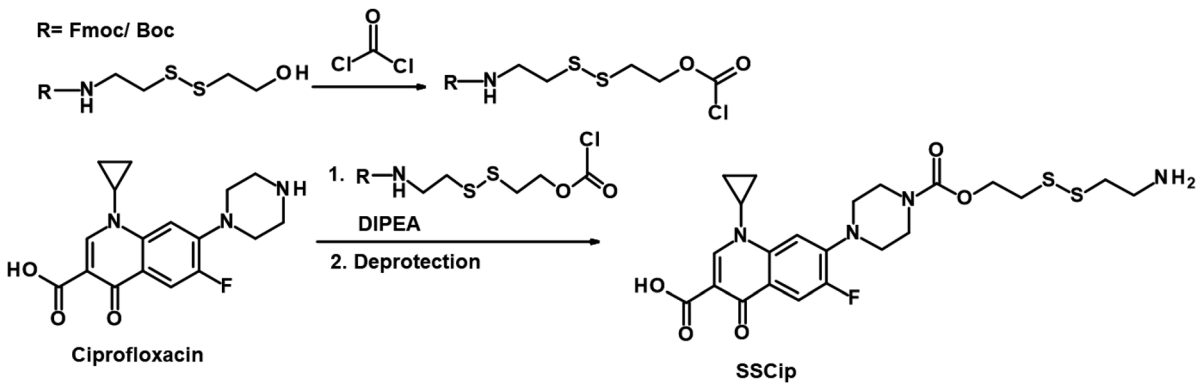

Fig. 2 Three-step synthesis of **SSCip** using Boc or Fmoc protective groups.

2.4. Synthesis of the chain transfer agent and functionalized initiator

The chain transfer agent *N*-(3-azidopropyl)-4-cyano-4-ethylsulfanyl-carbothioylsulfanyl-pentanamide (TTC-N_3) and the functionalized azoinitiator *N*-(3-azidopropyl)-4-[3-(3-azidopropylcarbamoyl)-1-cyano-1-methylpropylazo]-4-cyano-4-methylbutyramide (AIBIK-N_3) were prepared according to procedures described in the literature.[22,23]

2.5. Synthesis of polymers (P1–P3)

2.5.1. P1. Polymer precursor **P1** based on HPMA and Ma-β-Ala-TT was synthesized by RAFT (reversible addition–fragmentation chain-transfer) polymerization, using the functionalized CTA (chain transfer agent) TTC-N_3 and the azoinitiator AIBIK-N_3 in two steps as follows (Fig. 3). HPMA (700 mg, 4.89 × 10^{-3} mol) was dissolved in *t*-BuOH (6.2 mL) and added to Ma-β-Ala-TT (140 mg, 5.43 × 10^{-4} mol) dissolved in DMA (1 mL), giving a comonomer molar ratio of 90 : 10. The initiator AIBIK-N_3 (5.49 × 10^{-3} g, 1.23 × 10^{-5} mol) dissolved in DMA (225 μL) and the chain transfer agent TTC-N_3 (8.53 × 10^{-3} g, 2.47 × 10^{-5} mol) dissolved in DMA (225 μL) were then added (the molar ratio of monomer : CTA : initiator was 440 : 2 : 1). Prior to polymerization, the reaction mixture was bubbled with argon for 10 min. Polymerization was carried out under an inert atmosphere at 70 °C for 20 h. The reaction mixture was precipitated into an acetone : diethyl ether mixture (2 : 1), reprecipitated from methanol into the same mixture and dried under vacuum. Yield: 575 mg (68%).

To remove the terminal trithiocarbonate (TTC) groups, the precursor (575 mg) was dissolved in DMA (5 mL), and AIBIK-N_3 (120 mg, 2.67 × 10^{-4} mol) in DMA (750 μL) was added. Prior to the reaction, the mixture was bubbled with argon. The reaction was then carried out in a polymerization ampoule under an inert atmosphere at 80 °C for 3 h. After cooling, the product was precipitated into acetone : diethyl ether (2 : 1), reprecipitated from methanol into the same mixture and dried under vacuum. Yield: 550 mg (95%).

2.5.2. P2. Polymer precursor **P2** was obtained in two steps from **P1** (see Fig. 3). In the first step, precursor **P1** (200 mg, 1.2 × 10^{-4} mol TT) was dissolved in MeOH (1 mL) and added to a solution of DBCO–DFX (9.04 mg, 1.07 × 10^{-5} mol) dissolved in DMA (0.5 mL). After 0.5 h, the synthesized polymer containing the DFX group was precipitated into acetone : diethyl ether (2 : 1), reprecipitated from MeOH into the same mixture, and dried under vacuum.

The product (200 mg) was then redissolved in MeOH (2 mL), and $FeCl_3 \cdot 6H_2O$ (78.5 mg, 2.90 × 10^{-5} mol) was added. The solution immediately developed a dark-red color. The precursor, containing the DFX–Fe complex, was precipitated into diethyl ether, dried under reduced pressure, and finally purified by chromatography on a PD-10 column (Sephadex G-25, H_2O), followed by lyophilization.

2.5.3. P3. Control polymer **P3** was obtained from precursor **P2** (100 mg, 6 × 10^{-5} mol TT) dissolved in MeOH (1 mL) by reaction with 1-aminopropan-2-ol (10 μL, 1.28 × 10^{-4} mol). After 0.5 h, the polymer was precipitated into diethyl ether (20 mL), dried under vacuum, dissolved in water, purified on a PD-10 column and lyophilized. The procedure is depicted in Fig. 3.

2.6. Synthesis of polymer conjugates with ciprofloxacin bound *via* non-degradable linkage (PNC)

Polymer precursor **P1** was used for the preparation of non-targeted polymer–ciprofloxacin conjugates (**PNC** and **PC**), whereas precursor **P2** bearing terminal DFX–Fe units was employed for the synthesis of targeted conjugates (**PNC-Fe** and **PC-Fe**).

2.6.1. PNC. Ciprofloxacin (7.73 mg, 2.33 × 10^{-5} mol) was dissolved in DMF (4 mL) at 80 °C and subsequently mixed at 25 °C with precursor **P1** (76.6 mg, 4.6 × 10^{-5} mol TT) dissolved in methanol. After 12 h, 1-aminopropan-2-ol (10 μL, 1.28 × 10^{-4} mol) was added to block residual TT groups and the reaction mixture was stirred for an additional 30 min. The mixture was then evaporated to dryness, and the residue was dissolved in water and purified by size-exclusion chromatography (Sephadex G-25, H_2O). The procedure is depicted in Fig. 3. Yield: 80.3 mg (95%).

2.7. Synthesis of polymer conjugates with cleavable ciprofloxacin (PC)

2.7.1. PC. SSCip (7 mg, 1.37 × 10^{-5} mol) was dissolved in DMA (100 μL) and mixed with precursor **P1** (73.2 mg, 4.39 ×

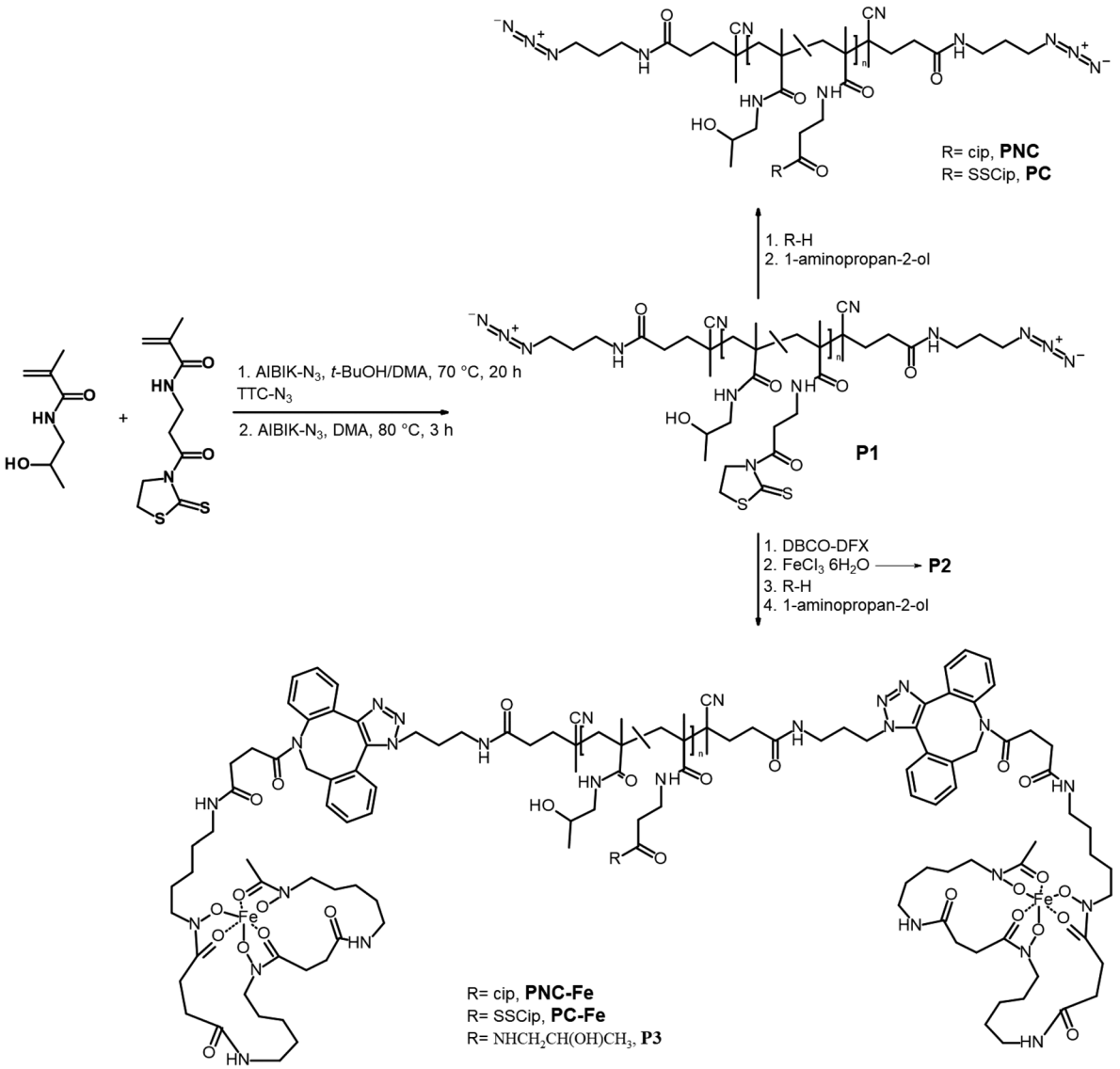

Fig. 3 Synthesis of polymers **P1–P3**, **PNC**, **PC**, **PNC-Fe** and **PC-Fe**.

10^{-5} mol TT) dissolved in DMA (100 μL). To convert the amino group of **SSCip** into the free base, DIPEA (4 μL, 2.3×10^{-5} mol) was added. After 1 h, 1-aminopropan-2-ol (6 μL, 7.68×10^{-5} mol) was introduced in order to block residual TT groups and the reaction mixture was stirred for an additional 30 min. The reaction mixture was precipitated into diethyl ether and dried under vacuum. The precipitate was redissolved in water, purified by size-exclusion chromatography (Sephadex G-25, H_2O) and lyophilized. The synthetic procedure is illustrated in Fig. 3. Yield: 78 mg (97%).

2.8. Synthesis of polymer conjugates with the targeting unit DFX–Fe

Targeted polymer–ciprofloxacin conjugates containing a DFX–Fe targeting unit were prepared in both cleavable (**PC-Fe**) and non-cleavable (**PNC-Fe**) variants.

2.8.1. PNC-Fe. Ciprofloxacin (5.46 mg, 1.65×10^{-5} mol) was dissolved in DMF (3 mL) at 80 °C and subsequently added at 25 °C to a solution of precursor **P2** (57.3 mg, 3.44×10^{-5} mol TT) in DMF (1 mL). After 12 h, 1-aminopropan-2-ol (5 μL, 6.4×10^{-5} mol) was added in order to block residual TT groups and the reaction mixture was stirred for an additional 30 min. The solvent was then evaporated, and the oily residue was dissolved in water, purified by size-exclusion chromatography (Sephadex G-25, H_2O) and lyophilized. The procedure is depicted in Fig. 3.

2.8.2. PC-Fe. SSCip (6 mg, 1.18×10^{-5} mol) was dissolved in DMA (85 μL) and added to a solution of precursor **P2** (56 mg) in MeOH (1.5 mL). To convert the amino group of **SSCip** into the free base, DIPEA (4 μL, 2.3×10^{-5} mol) was added. After 1 h, 1-aminopropan-2-ol (6 μL, 7.68×10^{-5} mol) was introduced in order to block residual TT groups and the

reaction mixture was stirred for an additional 30 min. The reaction mixture was then precipitated into diethyl ether and dried under vacuum. The precipitate was dissolved in water, purified by size-exclusion chromatography (Sephadex G-25, H_2O) and lyophilized. The procedure is depicted in Fig. 3.

2.9. Analytical methods and physicochemical characterization

2.9.1. High-performance liquid chromatography (HPLC). Analytical HPLC was performed using an LC-20 HPLC system (Shimadzu, Japan) equipped with a photodiode array detector (SPD-M20A) and a Chromolith® High Resolution RP-18e column. Elution was carried out using a linear gradient of mobile phase A (water/acetonitrile 95/5, v/v) and mobile phase B (acetonitrile/water 95/5, v/v), either with or without the addition of 0.1% trifluoroacetic acid (TFA), from 0 to 100% B at a flow rate of 4 mL min^{-1}. Analytical HPLC was used for monitoring reaction progress and for assessing the purity of the synthesized compounds.

Preparative HPLC was carried out using a PrepChrom C-700 flash chromatography system (Büchi, Switzerland) equipped with a photodiode array (PDA) detector. Separation was performed at a flow rate of 60 mL min^{-1} using a linear gradient from 0 to 100% B over 15 min (mobile phase A: water/acetonitrile 95/5, v/v; mobile phase B: acetonitrile/water 95/5, v/v). PDA detection was performed in the range of 200–400 nm. Preparative HPLC was employed for the isolation and purification of the disulfide ciprofloxacin derivative (**SSCip**).

2.9.2. Determination of molar masses and hydrodynamic diameters of the polymers. An HPLC system equipped with a photodiode array with a UV-VIS detector (SPD-M40, Shimadzu, Japan), a refractometric detector (Optilab, Wyatt, Germany), and an 18-angle static light scattering detector (DAWN II, Wyatt, Germany) was used for the analysis. The separation was performed on a Superose 6 Increase 10/300 GL column (GE Healthcare, Chicago, Illinois, USA) in 0.05 M phosphate buffer with 0.15 M NaCl (pH 7.4 at a flow rate of 0.5 mL min^{-1}). The measured data were processed using ASTRA 8.1 software (Wyatt) and LabSolutions 5.106 (Shimadzu). The refractive index increment value dn/dc was 0.167 mL g^{-1}.

Hydrodynamic particle diameter (D_H) of the samples **P1–3**, **PNC**, **PNC-Fe**, **PC** and **PC-Fe** was measured by dynamic light scattering (DLS) (Fig. S5) using a Zetasizer Ultra instrument (Malvern Panalytical, UK) at a laser wavelength of λ = 632.8 nm and a scattering angle of θ = 173°. The data were evaluated using ZS Xplorer software. All samples were measured at a concentration of 3.0 mg mL^{-1} in PBS (pH 7.4).

2.9.3. Determination of TT group content. The content of TT groups was determined spectrophotometrically from the absorbance of TT in DMSO using the Lambert–Beer law. A molar absorption coefficient of ε_{TT} = 11 400 L mol^{-1} cm^{-1} (λ_{max} = 305 nm) was applied for the calculation.

2.9.4. Determination of DFX and chelated iron content. The total DFX content on the polymer precursor was determined after the formation of the DFX–Fe complex in water. Polymer precursor **P2** (1 mg) and $FeCl_3 \cdot 6H_2O$ (13.1 mg) were dissolved in 1 mL of water, transferred to a cuvette, and the absorbance of the solution was measured at 432 nm immediately after mixing. A molar extinction coefficient of 26 966 L mol^{-1} cm^{-1} was used for the calculation.

Given the high chelating affinity of deferoxamine for iron and the large excess of $FeCl_3 \cdot 6H_2O$ used, it was assumed that the molar amount of bound DFX corresponded to the molar amount of complexed iron. This assumption was subsequently confirmed by elemental analysis performed by a service laboratory.

2.9.5. Determination of ciprofloxacin content. The conjugated ciprofloxacin content was determined using ^{1}H NMR in *d*6-DMSO using the following equation:

$$\frac{I_{Cip}}{I_{Cip} + I_{HPMA}} \times 100$$

where I_{Cip} is the integral of the ciprofloxacin proton signal at 8.68 ppm (s, 1H) and I_{HPMA} is the integral of the HPMA backbone signal at 4.7 ppm (br, 1H).

2.9.6. Determination of the release rate of ciprofloxacin. Polymer conjugates **PC** and **PC-Fe** (corresponding to 100 μM ciprofloxacin) were dissolved in 75 mM Tris-HCl buffer (pH 7.4) with 1 mM of GSH. The reaction mixture (450 μL) was incubated at 25 °C. At defined time intervals, 10 μL aliquots were withdrawn, and the reaction was quenched by adding 5 μL of 6% aqueous TFA. Ciprofloxacin release was monitored by HPLC (Fig. S6).

To determine 100% release, the same procedure was applied, replacing GSH with TCEP at equimolar concentrations. The reaction was monitored over time by HPLC. The peak area of ciprofloxacin at the point where no cleavage intermediates were detectable in the mixture was taken as 100% released ciprofloxacin. At early stages, additional peaks were observed, which gradually converted into a single peak corresponding to ciprofloxacin.

The procedure was adapted from the methodology described in ref. 24.

2.10. Biological characterization

2.10.1. Minimum inhibitory concentration (MIC). MIC is the lowest concentration of an antibacterial agent expressed in μg mL^{-1}, which, under strictly controlled *in vitro* conditions, completely prevents visible growth of the test strain of an organism.[25]

MIC was determined by microdilution of samples in liquid Mueller–Hinton broth (MH; 0.25 μg Fe mL^{-1} as quantified by Inductively Coupled Plasma Mass Spectrometry (ICP-MS)). An overnight culture of *S. aureus* CCM4516 and *E. coli* CCM4517 was aerobically cultivated in MH broth at 34 °C on a shaker (130 rpm) and was adjusted to 0.5 McFarland and diluted in MH broth to a final inoculum of 10^5 CFU mL^{-1}. The culture was seeded onto non-surface-treated 96-well plates (SPL, Korea), 100 μL per well. Samples of the ciprofloxacin derivatives were added (10 μL) in serial dilutions starting at 250 μg mL^{-1} of ciprofloxacin equivalent. Non-treated wells and wells treated with ampicillin (150 μg mL^{-1}) were used as controls.

Plates were incubated at 34 °C for 24 hours without shaking; then, absorbance at 600 nm (OD_{600}) was measured. MIC was determined as the concentration of the drug in wells with absorbance equal to that in control wells with ampicillin (with no visible bacterial growth). All tests were performed in triplicate in three independent experiments. Results are shown as means ± standard error. All MIC values for polymer conjugates are reported as ciprofloxacin-equivalent concentrations.

2.10.2. Cytotoxicity evaluation in human fibroblasts. To assess the cytotoxicity of **SSCip**, **Cip**, **PC**, **PC-Fe**, **PNC**, and **PNC-Fe**, a PrestoBlue assay (Invitrogen, Thermo Fisher Scientific) was performed using a human fibroblast cell line (HF; kindly provided by the Institute of Experimental Medicine of the Czech Academy of Sciences). The PrestoBlue assay is based on the reduction of resazurin to resorufin in metabolically active cells, enabling fluorescence-based quantification of cell viability.

HF cells were cultured in Dulbecco's modified Eagle's medium (DMEM; Gibco, Thermo Fisher Scientific) supplemented with 10% fetal bovine serum (FBS; Sigma-Aldrich) and 1% penicillin/streptomycin (P/S; Gibco, Thermo Fisher Scientific) at 37 °C under a humidified atmosphere containing 5% CO_2. Passages 3 to 10 are used for experiments. The cells were seeded in 96-well plates (4000 cells per well in 100 μL; TPP, Switzerland) and incubated overnight. Samples were added in serial dilutions (10 μL) starting with a concentration corresponding to 75 μg mL^{-1} of ciprofloxacin equivalents. Wells treated with PBS only served as untreated controls.

After 72 h of incubation, 10 μL of PrestoBlue reagent was added to each well, followed by incubation for an additional 4 h. Fluorescence was measured at an excitation wavelength of 560 nm and an emission wavelength of 590 nm using a Tecan Spark® microplate reader. Cell viability was expressed as a percentage relative to untreated control cells.

2.10.3. Macrophage infection with *E. coli* and evaluation of intracellular antibacterial activity. To assess the antibacterial activity of ciprofloxacin and its derivatives (**Cip**, **SSCip**, **PC**, **PC-Fe**, **PNC**, and **PNC-Fe**) against intracellular bacterial infection, a macrophage infection model using *E. coli* CCM4517 was employed. Murine alveolar macrophages MH-S (Sigma-Aldrich) were cultured in complete RPMI 1640 medium supplemented with 10% fetal bovine serum (FBS), 1% penicillin/streptomycin, 2 mM L-glutamine and 0.05 mM 2-mercaptoethanol at 37 °C under a humidified atmosphere containing 5% CO_2. *E. coli* CCM4517 was cultured overnight in Mueller–Hinton broth at 37 °C under aerobic conditions with shaking (120 rpm).

For the infection experiments, MH-S cells (passages 3 to 5) were seeded at a density of 2×10^5 cells per well in 500 μL of complete RPMI medium in 24-well plates and incubated overnight. The cells were subsequently infected with *E. coli* using 2×10^6 CFU per well, determining the initial multiplicity of infection (MOI) to be 10, in CO_2-independent medium supplemented with 5% FBS (without antibiotics) and incubated for 2 h at 37 °C. The infected cells were washed 3× with PBS and incubated for 1 h in 500 μL of CO_2-independent medium containing gentamicin (100 μg mL^{-1}) to eliminate extracellular bacteria. Cells were washed 3× in PBS and the medium was then replaced with 500 μL CO_2-independent medium supplemented with 5% FBS and gentamicin (2 μg mL^{-1}).

After 24 h, the medium was replaced with 500 μL of fresh CO_2-independent medium containing 5% FBS, and **Cip**, **SSCip**, **PC**, **PC-Fe**, **PNC**, or **PNC-Fe** was added at concentrations corresponding to 0.5×, 1×, and 2× MIC values determined as described above (see section 2.10.1). The plates were incubated for an additional 24 h at 37 °C in a CO_2-independent atmosphere. The cells were then washed 3× in PBS and lysed using 0.1% Triton™ X-100 for 10 min, and the resulting lysates were serially diluted and plated on Mueller–Hinton agar plates. After 24 h of incubation at 37 °C, the bacterial colonies were counted to determine the number of intracellular viable bacteria.

All experiments were performed in duplicate in three independent experiments.

Results were analyzed using GraphPad Prism software and are presented as the mean ± standard error of the mean (SEM) from at least three independent experiments. Statistical significance was defined as $P < 0.1$ (*) and $P < 0.05$ (**).

3. Results and discussion

The aim of the study was to design effective targeted polymer nanotherapeutics and to evaluate how the linker degradability and siderophore-mediated targeting influence the antibacterial activity against *S. aureus* and *E. coli*. We designed a series of HPMA-based polymer–ciprofloxacin conjugates differing in the linker degradability and in the presence of a DFX–Fe targeting unit.

3.1. Synthesis of the polymer precursors

The polymer precursor **P1** was synthesized by controlled RAFT polymerization of HPMA and Ma-β-Ala-TT using AIBIK-N_3 as the initiator and TTC-N_3 as the chain transfer agent, which enabled the introduction of a single azide group at the polymer chain end. The monomer : CTA : initiator ratio was selected to target a molar mass below the renal filtration threshold, thereby allowing renal clearance of the polymer carrier after fulfilling its function as a delivery vector *in vivo*. Removal of the TTC end group from the polymer chain was carried out by reaction with AIBIK-N_3, thereby introducing an azide function at the opposite chain end as well. Thus, a telechelic polymer with both main chain ends terminated with azide groups was formed. The polymer precursor was isolated in 68% yield and exhibited a molar mass and hydrodynamic radius (Fig. S5) consistent with the intended design for renal excretion (Table 1).

The targeting moiety was introduced into polymer precursor **P1** by attaching DFX–Fe units to the polymer chain ends, thus forming the polymer precursor **P2**. The DFX–Fe complex was selected because deferoxamine acts as a xenosiderophore, capable of promoting siderophore-mediated targeting and

Table 1 Physicochemical characterization of polymer precursors and polymer–ciprofloxacin conjugates

Sample	Cip content[a] (wt%)	M_n [b] (g mol^{-1})	$Đ$[b]	D_h [c] (nm)
P1	—	27 800	1.15	8.0
P2	—	25 000	1.42	9.0
P3	—	28 000	1.18	9.0
PNC	9.65	36 000	1.40	8.0
PNC-Fe	8.20	34 400	1.19	9.0
PC	3.09	31 400	1.24	10.0
PC-Fe	3.86	34 000	1.44	10.0

[a] Determined by ^{1}H NMR. [b] Determined by SEC/MALS in PBS. [c] Determined by DLS in PBS.

uptake across a broad spectrum of bacterial species. The targeting moieties were attached using the selective strain-promoted cycloaddition of terminal azide groups with DBCO–DFX, a reaction that proceeded rapidly and quantitatively under mild conditions. Subsequent addition of $FeCl_3{\cdot}6H_2O$ afforded the desired DFX–Fe complex, while careful purification ensured removal of the excess of iron. The course of the conjugation reaction was monitored by HPLC, which confirmed complete conversion within a short time frame. This synthetic approach thus provided stable, well-defined targeted precursor **P2** that could be further employed for covalent attachment of ciprofloxacin or its disulfide derivative. The functionality of the polymer precursor **P2** was determined spectrophotometrically based on the absorbance of the DFX–Fe complex and corresponded to an average of 1.7 targeting units per polymer chain. This is in accordance with the iron content of 0.028 wt% determined by elemental analysis. Introduction of the DFX–Fe targeting unit had only a minor effect on the molar mass and hydrodynamic radius of the conjugates (Table 1).

3.2. Synthesis of the polymer–Cip conjugate with a non-cleavable bond (PNC)

For the synthesis of polymer conjugates with ciprofloxacin attached through a non-cleavable bond, the TT groups of the polymer precursor **P1** were reacted with the secondary amino group of ciprofloxacin, resulting in conjugate **PNC** containing an amide linkage (Fig. 3). The reaction proceeded quantitatively but markedly slower due to the limited reactivity of the secondary amine, requiring an extended reaction time of 12 h. Such behavior is consistent with the steric and electronic properties of secondary amines, which generally reduce their reactivity compared with the primary analogues.

Determination of ciprofloxacin content by ^{1}H NMR spectroscopy in *d*6-DMSO confirmed successful conjugation and provided a value of 9.65 wt%, which is sufficient for the following biological evaluation. SEC–MALS analysis further demonstrated that conjugation had no significant effect on molar mass or hydrodynamic radius, both of which remained comparable to those of the polymer precursor (Table 1). These results demonstrate that the selected approach is suitable for the synthesis of amide-linked ciprofloxacin conjugates.

3.3. Design and synthesis of a disulfide-containing ciprofloxacin derivative (SSCip)

To enable controlled intracellular release of ciprofloxacin, a strategy based on the introduction of a reductively cleavable disulfide linker was pursued.[26] For this purpose, a ciprofloxacin derivative containing a disulfide bond (**SSCip**) was prepared, and the synthetic procedure was optimized to achieve high yield and suppress the formation of side products. The most efficient approach employed Boc-NH-SS as the starting material (see Fig. 2).

In this case, Boc-NH-SS was converted into the corresponding chloroformate by reaction of the hydroxy group with phosgene and, owing to the high reactivity of the intermediate, it was used directly without isolation. The resulting chloroformate reacted readily with ciprofloxacin, which had been converted to its free base by the addition of DIPEA. TMU was selected as the reaction solvent due to its inertness toward both phosgene and the chloroformate intermediate, allowing smooth progression of the coupling step. Subsequent removal of the Boc protecting group under acidic conditions using TFA did not promote splitting of the disulfide bond and therefore effectively suppressed the formation of the symmetric disulfide byproduct CipSSCip (Fig. S7 and S8). As a result, **SSCip** was obtained with a high overall yield of 70%. The structure and purity of **SSCip** were confirmed by ^{1}H NMR spectroscopy (Fig. S1).

For comparison, an alternative synthetic approach based on Fmoc-NH-SS was also examined. However, deprotection of the Fmoc group under alkaline conditions led to pronounced formation of the symmetric disulfide CipSSCip, resulting in a markedly lower yield of the target compound (17%). Consequently, this route was not pursued further.

3.4. Synthesis of the polymer–Cip conjugate with a cleavable bond (PC)

SSCip was subsequently used for the synthesis of the cleavable conjugate (**PC**). Reaction of the primary amino group of **SSCip** with TT groups along the polymer backbone proceeded much more rapidly than in the case of **PNC** – complete conversion was achieved within 1 h, as confirmed by HPLC monitoring (Fig. S4). The ciprofloxacin content in the resulting polymer conjugate **PC** was 3.09 wt%, as determined by ^{1}H NMR spectroscopy in *d*6-DMSO. SEC–MALS analysis further showed that the conjugation did not significantly alter the molar mass or hydrodynamic radius, both of which remained comparable to those of the polymer precursor (Table 1).

3.5. Synthesis of polymer–ciprofloxacin conjugates targeted with DFX–Fe

Using polymer precursor **P2** bearing terminal DFX–Fe units, two targeted polymer–ciprofloxacin conjugates were prepared, differing in the structure of the linker connecting ciprofloxacin to the polymer backbone. Ciprofloxacin was attached either *via* a non-cleavable amide bond (**PNC-Fe**) or through a reductively cleavable disulfide-containing linker using the **SSCip** derivative

(**PC-Fe**). The conjugation reactions were performed analogously to those of the corresponding non-targeted systems. Attachment of ciprofloxacin *via* its secondary amino group proceeded more slowly and required extended reaction times, whereas conjugation of **SSCip**, bearing a primary amino group, was significantly faster.

Importantly, incorporation of the DFX–Fe targeting unit did not adversely affect the efficiency of conjugation, nor did it lead to pronounced changes in molar mass, dispersity, or hydrodynamic radius of the resulting conjugates (Table 1).

These results indicate that the DFX–Fe targeting motif can be incorporated into both cleavable and non-cleavable polymer–ciprofloxacin conjugates without compromising their physicochemical characteristics, thereby enabling subsequent evaluation of the influence of the targeting on antibacterial activity.

3.6. Release of ciprofloxacin from conjugates PC and PC-Fe

Release studies under reducing conditions (1 mM GSH, pH 7.4) revealed marked differences between the cleavable polymer–ciprofloxacin conjugates **PC** and **PC-Fe**. As shown in Fig. 4, **PC** exhibited a faster and more complete release of ciprofloxacin, whereas incorporation of the DFX–Fe targeting unit significantly slowed down the release process and reduced the fraction of ciprofloxacin liberated in its native form. These data confirm that the disulfide linker is chemically cleavable under reductive conditions, while simultaneously indicating that the presence of Fe^{3+} alters the release kinetics.

To clarify the origin of this behavior, the formation of disulfide-containing byproducts during the release process was examined (Fig. 5). In parallel with the slowed release of **Cip** observed for **PC-Fe**, a pronounced formation of the symmetric disulfide derivative CipSSCip was detected, whereas it was considerably less pronounced in the absence of iron. This observation indicates that Fe^{3+} promotes oxidative disulfide scrambling, thereby diverting a fraction of the released thiol intermediates into side reactions (Fig. S6). Given the low solubility of CipSSCip, its formation effectively decreases the amount of ciprofloxacin available in the solution within the applied model system.

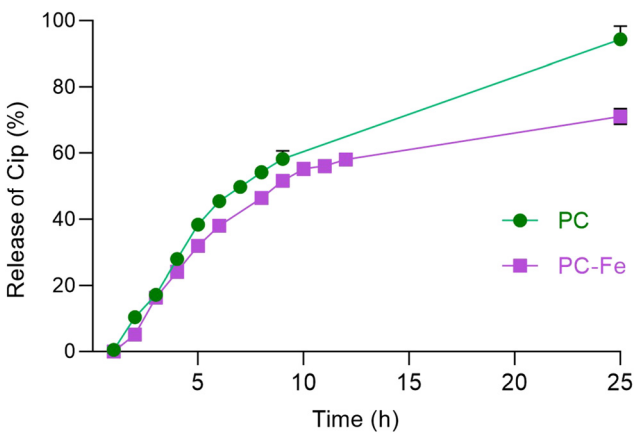

Fig. 4 Time-dependent release of ciprofloxacin from **PC** and **PC-Fe** conjugates under reducing conditions (1 mM GSH, pH 7.4).

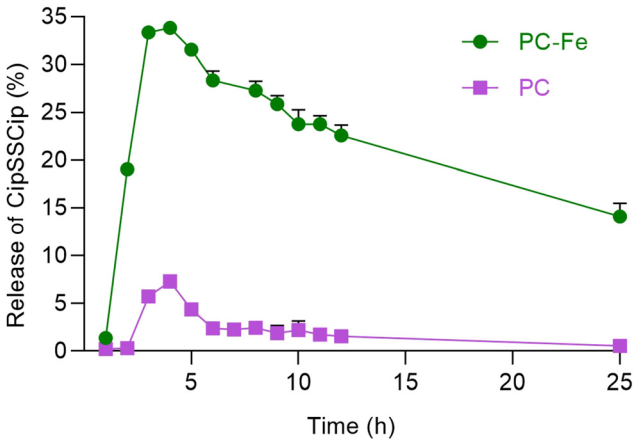

Fig. 5 Time-dependent formation of the disulfide byproduct CipSSCip during reductive cleavage of **PC** and **PC-Fe** conjugates in the presence of 1 mM GSH (pH 7.4).

It should be emphasized that these release experiments were conducted under static *in vitro* conditions, which serve as a simplified model to probe linker cleavability and potential side reactions. In dynamic biological environments, where continuous transport, compartmentalization, and regulated redox processes occur, the extent to which such iron-mediated side reactions contribute to the overall release profile may differ. Nevertheless, the combined analysis of ciprofloxacin release kinetics (Fig. 4) and byproduct formation (Fig. 5) demonstrates that, beyond linker degradability, the redox activity associated with targeting motifs can influence drug release pathways and should therefore be considered in the design of targeted polymer conjugates.[24]

3.7. Antibacterial activity of the polymer–ciprofloxacin conjugates

The antibacterial activity of the prepared polymer–ciprofloxacin conjugates was evaluated in order to elucidate the influence of the chemical nature of the linkage between the polymer carrier and the drug, as well as the effect of the presence of the DFX–Fe targeting unit, on the resulting efficacy against *E. coli* and *S. aureus* (Fig. 6).

Comparison of the polymer conjugates bearing a non-cleavable (**PNC**) and a cleavable linkage (**PC**) demonstrates that the introduction of a reductively cleavable disulfide linker has a decisive impact on antibacterial activity. While **PNC** exhibited only limited activity against *E. coli* and was ineffective against *S. aureus* within the tested concentration range, the cleavable conjugate **PC** showed markedly enhanced activity against both bacterial strains (Fig. 6A and C).

These results clearly demonstrate that the mere presence of ciprofloxacin covalently bound to a polymer carrier through a non-cleavable amide bond is not sufficient to retain its biological function. The secondary amine of ciprofloxacin, which in

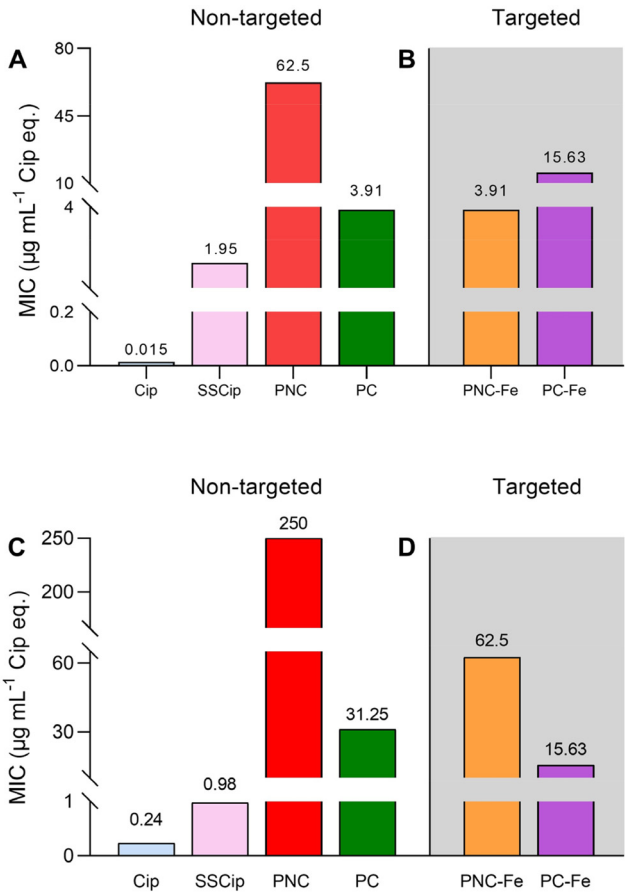

Fig. 6 Minimum inhibitory concentrations (MIC) of polymer conjugates against *E. coli* (A and B) and *S. aureus* (C and D). (A and C) Comparison of free ciprofloxacin (Cip), disulfide derivative (**SSCip**), non-cleavable conjugate (**PNC**), and cleavable conjugate (**PC**). (B and D) Targeted conjugates bearing DFX–Fe at polymer chain ends (**PNC–Fe**, **PC–Fe**).

the case of **PNC** is involved in conjugation to the polymer backbone, plays a critical role in the mechanism of action of the antibiotic, as it participates in the interaction with its enzymatic target, DNA gyrase. Blocking this functional group by the formation of an amide bond prevents proper binding of ciprofloxacin to the enzyme and thereby suppresses its inhibitory activity.[27,28] In contrast, incorporation of a disulfide linker enables regeneration of native ciprofloxacin under reductive conditions, which is consistent with the results of the release studies.

Introduction of the DFX–Fe targeting unit into the non-cleavable conjugate resulted in enhanced antibacterial activity. While **PNC** was active against *E. coli* only at higher concentrations and showed no detectable activity against *S. aureus*, the targeted conjugate **PNC-Fe** exhibited measurable activity against both bacterial strains within the tested concentration range (Fig. 6B and D). This observation indicates that the presence of the targeting unit can partially compensate for the absence of a cleavable linker.

Importantly, the polymer precursor **P3** bearing only terminal DFX–Fe units but no bound ciprofloxacin did not exhibit any antibacterial activity against either bacterial strain within the tested concentration range (data not shown), confirming that the observed activity originates from ciprofloxacin rather than from the targeting unit itself.

A different trend was observed for the cleavable conjugates. Although non-targeted polymer conjugate **PC** exhibited high antibacterial activity against *E. coli*, incorporation of the DFX–Fe unit led to a reduced efficacy of **PC-Fe** compared to its non-targeted analogue (Fig. 6B). This effect correlates with the release experiments, which demonstrated that the presence of Fe^{3+} slows down reductive cleavage of the disulfide linker and promotes the formation of the poorly soluble disulfide byproduct CipSSCip. As a result, the fraction of free ciprofloxacin available during static *in vitro* testing is reduced, leading to lower apparent antibacterial activity of **PC-Fe** against *E. coli*.

In contrast, for *S. aureus*, the activity of **PC-Fe** was slightly higher than that of **PC** (Fig. 6D). This difference may be attributed to differences in the intracellular redox environment between the two bacterial species. While *E. coli* contains high intracellular levels of glutathione, *S. aureus* lacks glutathione, which may result in different kinetics of disulfide cleavage and a reduced contribution of the competing oxidative side reactions.

It should be emphasized that both the release and biological experiments were performed under simplified static conditions, which do not fully reflect the dynamic environment of a living system. Therefore, it cannot be excluded that under biologically relevant conditions, the observed side processes would occur to a lesser extent or might not be dominant.

3.8. Activity against intracellular *E. coli* in infected macrophages

While MIC assays provide a basic comparison of antibacterial activity, the macrophage infection model enables the evaluation of bactericidal efficacy under conditions more closely resembling intracellular infections (Fig. 7). In this model, antibacterial activity was expressed as the percentage of surviving intracellular *E. coli* cells, which functionally corresponds to an assessment of minimal bactericidal concentration (MBC). All samples were tested at concentrations corresponding to 0.5×, 1×, and 2× their respective MIC values.

For all systems, a clear concentration-dependent antibacterial response was observed, with the lowest efficacy generally detected at 0.5× MIC. This trend confirms that intracellular antibacterial activity remains dose-dependent even in the complex cellular environment of macrophages. An exception was observed for the disulfide derivative **SSCip**, which exhibited antibacterial activity at 0.5× MIC comparable to that at MIC. This behavior can likely be attributed to its chemical structure, particularly the presence of a primary amino group, which may facilitate cellular uptake and enhance intracellular availability of the antibiotic.

Comparison of the polymer conjugates clearly demonstrates the critical role of the linker. The cleavable conjugate **PC** exhibited higher efficacy at elevated concentrations than its non-cleavable analogue **PNC**, confirming the importance of controlled intracellular release of ciprofloxacin. At the same

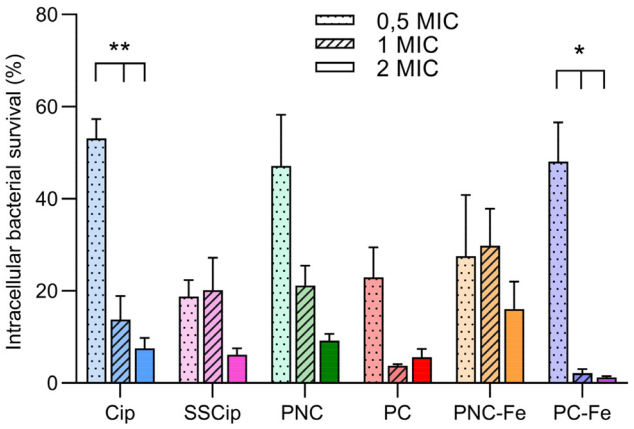

Fig. 7 Intracellular antibacterial activity of ciprofloxacin (**Cip**), its disulfide derivative (**SSCip**), non-cleavable polymer conjugates (**PNC** and **PNC-Fe**), and cleavable polymer conjugates (**PC** and **PC-Fe**) in an *E. coli*-infected macrophage model (MH-S cells). Data are expressed as the percentage of surviving intracellular bacteria relative to the untreated control (100%). Samples were tested at concentrations corresponding to 0.5×, 1×, and 2× MIC values determined against planktonic *E. coli*. Values represent mean ± SEM from three independent experiments performed in duplicate.

time, the most important finding of this study is that, at concentrations corresponding to MIC, all tested samples exhibited very similar antibacterial efficacy. This result provides key validation of the determined MIC values and demonstrates that they also correspond to biologically relevant concentrations in the intracellular infection model.

It is essential to emphasize that the absolute concentrations of ciprofloxacin at MIC differed substantially between individual systems due to their distinct MIC values. For example, the non-cleavable conjugate **PNC** exhibited an MIC of 62.5 μg mL^{-1}, whereas its targeted analogue **PNC-Fe** showed an MIC of only 3.91 μg mL^{-1}. Despite exhibiting comparable intracellular efficacy at their respective MICs, the ciprofloxacin concentration in the case of **PNC-Fe** was approximately 16-fold lower. This result unequivocally confirms the functionality of DFX–Fe-mediated targeting and demonstrates that active targeting enables a pronounced increase in efficacy at a substantially reduced antibiotic dose.

In the case of the cleavable conjugate **PC**, however, the introduction of the DFX–Fe targeting unit did not result in a comparably pronounced enhancement of efficacy, indicating that the cleavable linker alone already ensures highly efficient intracellular release of ciprofloxacin. Nevertheless, the combination of a cleavable linker and active targeting led to the highest overall efficacy among all tested systems. The **PC-Fe** conjugate was the most effective sample, and at a concentration corresponding to 1× MIC, the survival of intracellular *E. coli* cells was reduced to approximately 2%; more interestingly, at 2× MIC, the survival of intracellular *E. coli* cells was further reduced to approximately 1%. Only **Cip** and the **PC-Fe** conjugate showed a significant difference in efficiency between concentrations (Cip $P < 0.05$, **PC-Fe** $P < 0.1$).

Overall, these results demonstrate that MIC values alone do not provide a complete picture of the intracellular behavior of polymer–ciprofloxacin conjugates. At the same time, they confirm the validity of MIC determination and highlight the critical influence of both linker design and targeting units on biological efficacy across different antibiotic doses.

3.9. Cytotoxicity toward human fibroblasts

The cytotoxicity of Cip, its disulfide derivative (**SSCip**), polymer conjugates (**PNC** and **PC**), their DFX–Fe-targeted counterparts (**PNC-Fe** and **PC-Fe**), and the polymer control **P3** was evaluated using a human fibroblast cell line (Fig. 8). Cell viability was assessed by the PrestoBlue assay after 72 h of incubation over a

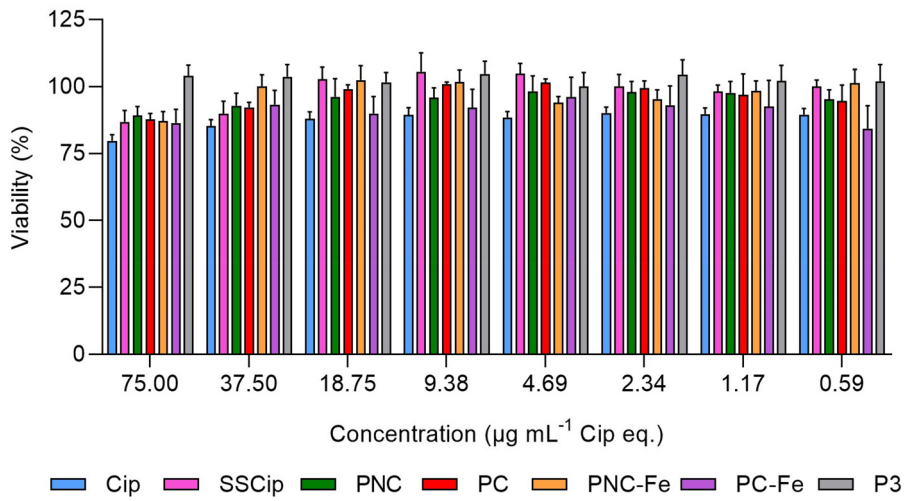

Fig. 8 Cytotoxicity of Cip, its disulfide derivative (**SSCip**), polymer conjugates (**PNC** and **PC**), their DFX–Fe-targeted counterparts (**PNC-Fe** and **PC-Fe**), and the polymer control **P3** toward human fibroblasts, evaluated using the PrestoBlue assay after 72 h of incubation. Cell viability is expressed as a percentage relative to untreated control cells. Ciprofloxacin concentrations are given as ciprofloxacin equivalents. Data are presented as mean ± SEM from three independent experiments (n = 3).

concentration range corresponding to ciprofloxacin or equivalents.

Across the entire tested concentration range, all samples exhibited high cell viability, with values remaining above 80%, which is commonly considered a threshold for non-cytotoxic behavior. No dose-dependent decrease in viability was observed for any of the polymer conjugates, including the targeted DFX–Fe systems. Notably, the polymer precursor **P3** bearing only the targeting unit also showed no detectable cytotoxicity, confirming that neither the polymer carrier nor the DFX–Fe moiety adversely affects fibroblast viability.

These results demonstrate that the introduction of ciprofloxacin, disulfide linkers, and DFX–Fe targeting units does not induce cytotoxic effects toward human fibroblasts under the tested conditions. The favorable cytocompatibility of all investigated systems supports their further investigation as antibacterial nanotherapeutics, particularly with respect to applications requiring prolonged circulation and repeated exposure.

4. Conclusion

In this work, we successfully designed, synthesized and evaluated a series of functional HPMA-based polymer–ciprofloxacin conjugates. A cleavable linker strategy enabled the controlled release of ciprofloxacin in its chemically unmodified and biologically active form, confirming the applicability of this approach for targeted antibiotic delivery. Furthermore, we showed that siderophore-mediated targeting *via* the DFX–Fe complex can enhance antibacterial efficacy under selected conditions, with both linker chemistry and bacterial strain playing critical roles. The combination of DFX–Fe targeting and cleavable linker chemistry has potential in the "realistic" *in vivo* setup. Such polymer nanomedicines showed promising activity against intracellular *E. coli* in infected macrophages even at a concentration equal to the MIC determined on the bacterial strain *in vitro*.

Although the polymer conjugates exhibited lower antibacterial activity in standard MIC assays compared to free ciprofloxacin, this observation reflects the intrinsic design of polymer-based systems rather than a limitation. The principal benefits of these conjugates are expected to manifest *in vivo*, particularly through prolonged circulation, enhanced accumulation at sites of inflammation or infection, and the potential to reduce dosing frequency due to sustained drug availability. Moreover, a moderated antibacterial effect may represent a therapeutic advantage in severe systemic infections, where excessively rapid bacterial lysis can trigger undesirable inflammatory responses. Overall, this study delineates key structure–activity relationships governing targeted polymer–antibiotic conjugates and provides a foundation for their further development toward *in vivo* applications.

Author contributions

A. Stehlíková carried out the synthesis of the polymer conjugates, performed their characterization, evaluated the data, and wrote the original draft of the manuscript. L. Kotrchová contributed to the characterization of the materials and compounds. M. Pechar participated in data evaluation and manuscript writing. K. Gunár performed the antibacterial activity studies. E. Rydvalová carried out the cytotoxicity experiments. M. Studenovský contributed to the synthesis. T. Etrych supervised the project.

Conflicts of interest

There are no conflicts to declare.

Data availability

The supporting data has been provided as part of the Supplementary information. Supplementary information: Figures with NMR spectra, ESI-MS spectra, HPLC chromatograms and structures, see DOI: https://doi.org/10.1039/d6bm00145a.

Acknowledgements

The authors gratefully acknowledge Barbora Koutníková for her technical support.

References

1 J. O'Neill, *Tackling Drug-Resistant Infections Globally: Final Report and Recommendations, The Review on Antimicrobial Resistance, London*, 2016, available at: https://amr-review.org/sites/default/files/160518_Final%20paper_with%20cover.pdf, (accessed January 2026).
2 World Health Organization, *Global Research Agenda for Antimicrobial Resistance in Human Health*, WHO, 2023, available at: https://www.who.int/publications/i/item/9789240071966 (accessed January 2026).
3 C. L. Ventola, *Pharm. Ther.*, 2015, **40**, 277.
4 J. Kopeček, *Adv. Drug Delivery Rev.*, 2013, **65**, 49–59.
5 R. Laxminarayan, A. Duse, C. Wattal, A. K. M. Zaidi, H. F. L. Wertheim, N. Sumpradit, E. Vlieghe, G. L. Hara, I. M. Gould, H. Goossens, C. Greko, A. D. So, M. Bigdeli, G. Tomson, W. Woodhouse, E. Ombaka, A. Q. Peralta, F. N. Qamar, F. Mir, S. Kariuki, Z. A. Bhutta, A. Coates, R. Bergstrom, G. D. Wright, E. D. Brown and O. Cars, *Lancet Infect. Dis.*, 2013, **13**, 1057–1098.
6 J. P. Patil, H. S. Mahajan and R. C. Patel, *Int. J. Pharma Sci. Res.*, 2015, **6**, 4611–4621.
7 J. Kopeček and J. Yang, *Adv. Drug Delivery Rev.*, 2020, **156**, 40–64.
8 L. Kostka, L. Kotrchová, V. Šubr, A. Libánská, C. A. Ferreira, I. Malátová, H. J. Lee, T. E. Barnhart, J. W. Engle, W. Cai, M. Šírová and T. Etrych, *Biomaterials*, 2020, **235**, 119728.
9 Z. Deng, J. Hu and S. Liu, *Macromol. Rapid Commun.*, 2020, **41**, 1900531.

10 G. G. Zhanel, A. Walkty, L. Vercaigne, J. A. Karlowsky, J. Embil, A. S. Gin and D. J. Hoban, *Can. J. Infect. Dis.*, 1999, **10**, 207–238.
11 A. M. Emmerson and A. M. Jones, *J. Antimicrob. Chemother.*, 2003, **51**, 13–20.
12 J. M. Blondeau, *Surv. Ophthalmol.*, 2004, **49**, S73–S78.
13 K. J. Aldred, R. J. Kerns and N. Osheroff, *Biochemistry*, 2014, **53**, 1565–1574.
14 I. Ekladious, Y. L. Colson and M. W. Grinstaff, *Nat. Rev. Drug Discovery*, 2019, **18**, 273–294.
15 G. Winkelmann, in *Biochemical Society Transactions*, Portland Press, 2002, vol. 30, pp. 691–696.
16 M. Miethke and M. A. Marahiel, *Microbiol. Mol. Biol. Rev.*, 2007, **71**, 413–451.
17 M. Petrik, E. Umlaufova, V. Raclavsky, A. Palyzova, V. Havlicek, J. Pfister, C. Mair, Z. Novy, M. Popper, M. Hajduch and C. Decristoforo, *Eur. J. Nucl. Med. Mol. Imaging*, 2021, **48**, 372–382.
18 G. S. Tillotson, *Infect. Dis.: Res. Treat.*, 2016, 45–52, DOI: 10.4137/idrt.s31567.
19 B. Rayner, A. D. Verderosa, V. Ferro and M. A. T. Blaskovich, *RSC Med. Chem.*, 2023, **14**, 800–822.
20 J. M. Varghese, J. A. Roberts and J. Lipman, *Crit. Care Clin.*, 2011, **27**, 19–34.
21 V. Šubr, L. Kostka, J. Plicka, O. Sedláček and T. Etrych, *Polymers*, 2024, **16**, 758.
22 V. Šubr, T. Ormsby, P. Šácha, J. Konvalinka, T. Etrych and L. Kostka, *Polym. Chem.*, 2021, **12**, 6009–6021.
23 V. Šubr, L. Kostka, J. Strohalm, T. Etrych and K. Ulbrich, *Macromolecules*, 2013, **46**, 2100–2108.
24 R. Pola, E. Grosmanová, M. Pechar, L. Kostka, E. Pokorná, L. Tušková, P. Klener and T. Etrych, *Polymers*, 2025, **17**, 2837.
25 I. Phillips, *Clin. Microbiol. Infect.*, 1998, **4**, 291–296.
26 W. Neumann and E. M. Nolan, *J. Biol. Inorg. Chem.*, 2018, **23**, 1025–1036.
27 V. Khwaza, S. Mlala and B. A. Aderibigbe, *Int. J. Mol. Sci.*, 2024, **25**, 4919.
28 G. F. Zhang, X. Liu, S. Zhang, B. Pan and M. L. Liu, *Eur. J. Med. Chem.*, 2018, **146**, 599–612.